The Effect of Stiffness of Supporting System on the Behaviour of Steel-Concrete Composite Beams at Elevated Temperature

Priya S. Natesh[1](✉) and Anil Agarwal[2]

[1] IcfaiTech (FST), ICFAI Foundation for Higher Education (Declared as Deemed to be University u/s 3 of the UGC Act 1956), Hyderabad 501 203, India
priyas@ifheindia.org

[2] Indian Institute of Technology, Hyderabad 502 285, India
anil@ce.iith.ac.in

Abstract. There are many knowledge gaps to be addressed in the behaviour of structural members under fire conditions. The behaviour of steel-concrete composite beams under the cooling phase is yet to be explored in-depth. In this paper, all the beam models are heated for an hour and the behaviour of composite beam systems in heating and cooling phases has been studied. The parameters considered for the present study are the axial stiffness of the supporting system of the composite beam and influence of the reinforcement at the support. A 3D finite element model of long span composite beam was developed using Abaqus software. The modelling technique and analysis procedure was validated with the literature. The length of the beam considered for parametric study was around 13 m. All models had simple shear connections. A parametric study was conducted to understand the influence of reinforcement at the beam ends, and the effect of support conditions provided for these reinforcements. The axial restraint provided at beam-ends were found to have a significant role in the behaviour of the beam under fire loading. Stiff connections are not preferable during the cooling phase of loading.

Keywords: Composite beam · Fire · Supporting system · Stiffness

1 Introduction

The optimum design can be achieved in composite beam offers with a structural steel beam in its tension zone concrete slab in its compression zone. The shear tab connection in the beam provides an adequate bond between the steel beam and the concrete slab. Normally the concrete slab can be of trapezoidal shape or flat shape in cross-section. At present, there is a substantial need of understanding the long-span composite beam behaviour under various accidental loadings such as impact, blast and fire. There are

J. A. Fonseca de Oliveira Correia et al. (Eds.): ASMA 2021, STIN 26, pp. 108–124, 2023.
https://doi.org/10.1007/978-3-031-05509-6_9

numerous yet limited experimental research works in the behaviour of composite beams under fire loading. Wainman et al. (1987), Zhao et al. (1997), Cedeno et al. (2009), Selden et al. (2015), Fischer et al. (2017), and Choe et al. (2018) are the researchers who performed experimental investigation on composite beams with simple shear connections under elevated temperatures. The experimental investigation of the behaviour of any structural members under fire loading and post-fire loading is costly, which demand alternative methods such as simulations using powerful software tools. Numerical model validated with experimental data can be used for such extensive study.

Wainman et al. (1987) performedan experimental investigation on the behaviour of the simply supported composite beam with a span of around 4.6 m under fire loading. The width and depth of the flat slab in the experimental setup were 0.642 m and 0.130 m, respectively. The authors concluded that at elevated temperature, the flexural failure happened once it reaches its plastic capacity. Zhao et al. (1997) focused on the importance of steel protection and slab width in composite beam behaviour by carrying out experimental investigation on 4.9 m long beams. IPE300 steel beam and a flat concrete slab were used. 19 mm diameter shear studs were used to connected the steel beam with the concrete slab. The mode of failure observed for the protected composite beam was crushing of concrete, and unprotected beams failed due to the plastification of steel member.

Agarwal et al. (2011, 2014) studied the behaviour of 10 storey office buildings under corner fire loading and the significance of shear tab connection in the stability of the building. Fischer et al. (2015, 2016, 2017) developed a numerical model and studied the behaviour of composite beams and connections in single-bay and three-bay systems. The connections considered were single-angle, double angle and shear tab. The fire protection, cooling rates were some of the parameters considered. With two-hour fire protection on steel beam, there was no tensile axial force developed in the member and no damage was observed. The connections with slotted hole and coped beam had large rotation and midspan deflections. Selden et al. (2015) studied the composite beam behaviour under fire loading and analysed the performance of simple shear connections. Partial composite beams having an effective span of 3.7 m were considered for the analysis. The authors found that for flat slabbed composite beam subjected to medium temperature, the potential mode of failure observed was compression failure. The authors concluded that the composite beam behaviour during the cooling phase is very significant as shear tab fracture was observed in the cooling phase of loading.

Choe et al. (2018) performed an experimental investigation of steel-concrete composite beams with simple shear double-angle connections. They considered long span simply supported and continuous beams with a span of 12.3 m subjected to gravity loading and thermal loading. The test protocol provides a very useful data such as the axial force in negative reinforcement and axial restraint force on the beam throughout the testing. Very few experiments provide such detailed data. Using the test data from this experiment, a detailed parametric study has been conducted to study the influence of various parameters on the behaviour and enhance the long-span continuous composite beam. The authors studied the influence of slab continuity. They observed that buckling of steel beam near the connection causes tensile force demand in continuity bars.

In the present paper, the fire and post-fire behaviour of a complex continuous composite beam using Abaqus software is studied. The modelling protocol was benchmarked with experimental data from the literature.

2 Modelling Approach

For simulation purpose, Abaqus software with FEM-based computer programme was selected. The structural behaviour under fire conditions is studied by first loading, the member with vertical loads and then the thermal loading was applied. The temperature history of each node is calculated beforehand. Therefore, the analysis was conducted in two parts. The first part of analysis was nonlinear heat transfer analysis was carried out first to get the time versus temperature of every node in the beam model. Furthermore, the second part was stress analysis with the dynamic explicit procedure to predict the effect of vertical load and fire load.

2.1 Heat Transfer

The 3D finite element model was developed in Abaqus using the DC3D8 element type, eight noded brick elements. Furthermore, a 3D heat transfer analysis was conducted on the entire system. The literature defined fire scenarios, and material properties were considered for benchmarking the analysis and modelling procedures. The same fire scenario and loading conditions were followed for parametric study as well. The default option available in the software for conducting heat transfer analysis was conduction. A user-defined subroutine from Cedeno et al. (2009) was adopted to incorporate convection and radiation as part of heat transfer analysis. All parts of the composite beam such as steel beam, metal deck, concrete slab, insulation materials, shear studs, wire mesh, rebars, angles and bolts were modelled using 3D brick elements.

2.2 Stress Analysis

The structural analysis was performed in the software in two steps. The first step was applying vertical load and the second one was the application of fire load. The second step included heating and cooling phases. The output file of heat transfer analysis was defined as a predefined load in the thermal load step as fire loading, which is possible only if the structural and heat transfer analysis models are compatible. Therefore, a 3D 8-node linear brick element with reduced integration and hourglass control, C3D8R, was used for stress analysis modelling purpose. Through mesh convergence study, mesh size of 35 mm has been finalised. Dynamic Explicit analysis procedure was adopted to predict this time-dependent behaviour of composite beam. The welding between the steel beam and shear stud was modelled using a tie, and the shear stud- concrete bond was defined using embedded constraint in the interaction module unit of Abaqus. In the interaction module, penalty contact was used to define surface to surface contact. The

contact between rebars and concrete and wire mesh and concrete were defined using embedded modelling. Displacement boundary conditions were defined for modelling the end conditions of sacrificing plates. Figure 1 shows the isometric view of the beam model in Abaqus.

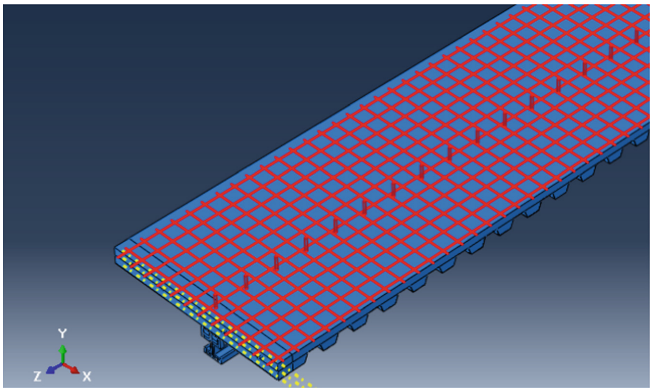

Fig. 1. Isometric view in Abaqus.

2.3 Material Properties

Eurocode defined temperature dependant material properties were adopted in the analysis. Thermal property such as, thermal expansion, conductivity, specific heat was also taken from the Eurocode.

2.3.1 Steel

From the published experimental works of literature, the yield strength of taken as the inputs for Eurocode distinct relationships for mechanical properties. For both steel and concrete models, temperature-dependent strength reduction factors from the code taken care of reduction in strength at elevated temperature. Figure 2 shows the Eurocode defined temperature dependent mechanical and thermal properties of steel.

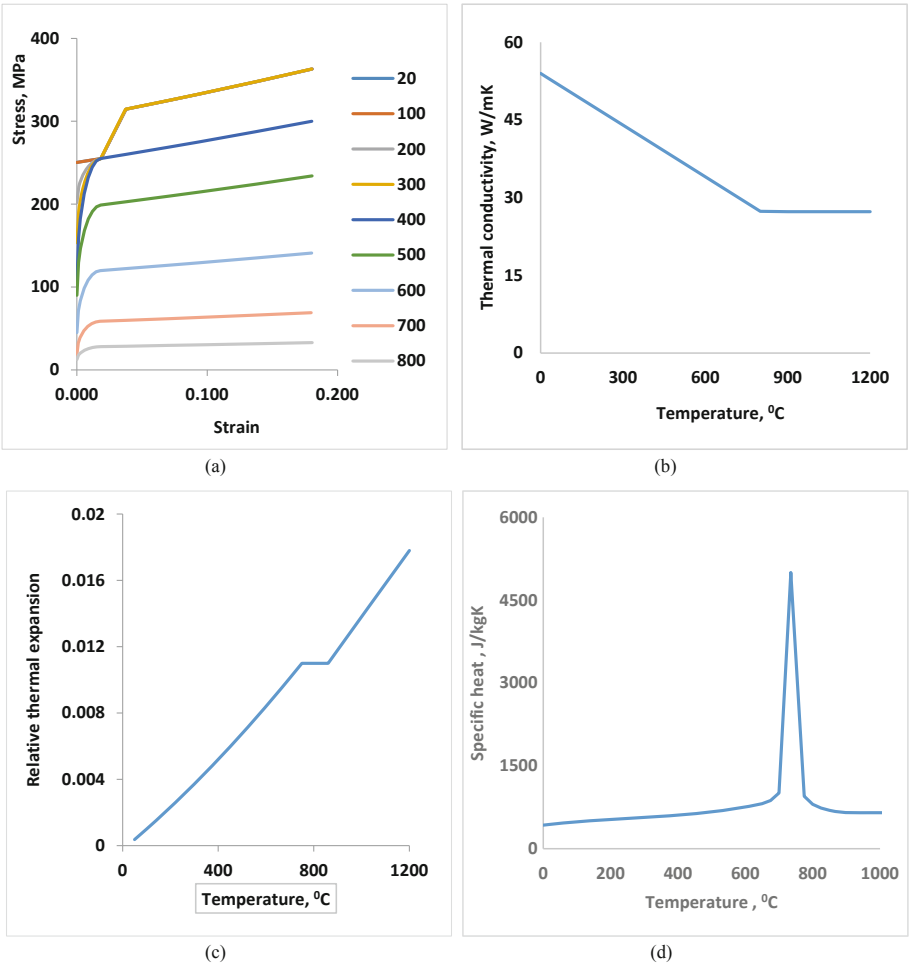

Fig. 2. (a) Stress-strain curve for steel (b) Thermal conductivity of steel (c) Relative thermal expansion of steel (d) Specific heat of steel.

2.3.2 Concrete

Drucker Prager plasticity model was used for simulating damage in concrete. Characteristic compressive strength of concrete for various models was taken from experimental data provided in the literature. Figure 3(a) to (d) show the typical Eurocode stress-strain curve for concrete with characteristic compressive strength of 28 MPa, thermal conductivity, thermal expansion and specific heat as a function of temperature. Specific heat of concrete with 3% moisture content adopted for modelling purpose as shown in Fig. 3(c).

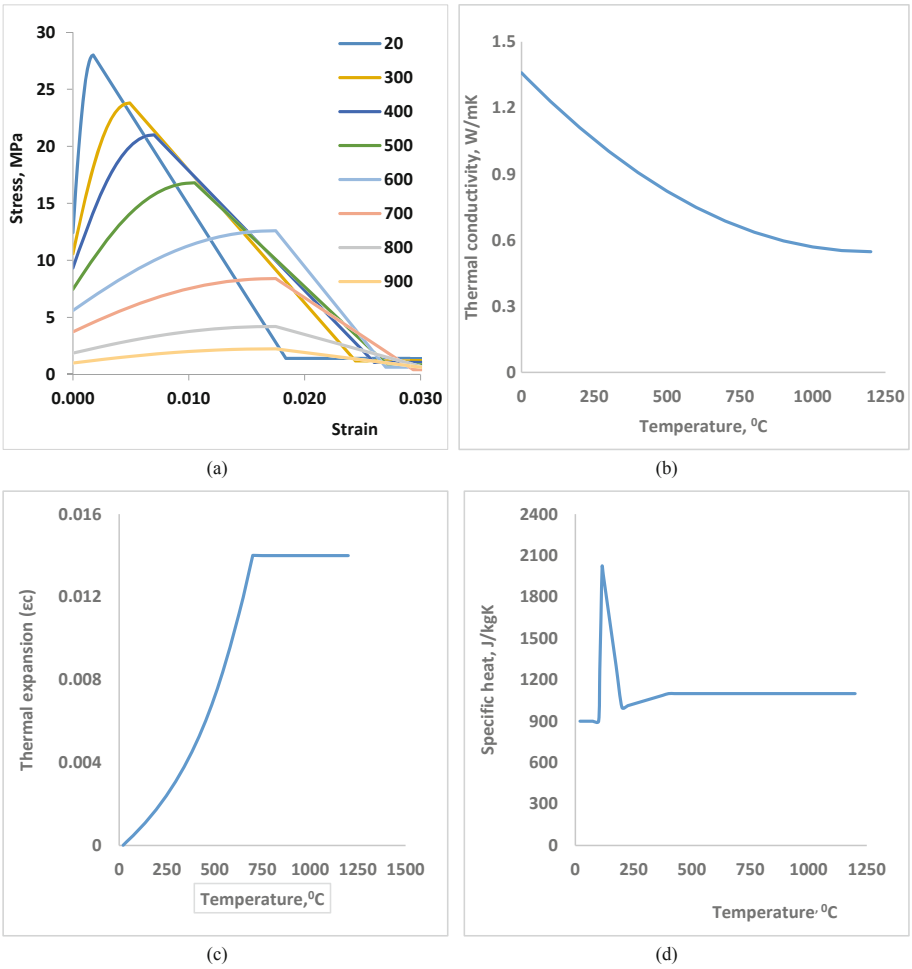

Fig. 3. (a) Stress-strain curve for concrete (b) Thermal conductivity of concrete (c) Thermal expansion of concrete (d) Specific heat of concrete.

3 Benchmarking of Modelling and Analysis

The analysis procedure adopted in this numerical investigation was benchmarked with the literature data. Experiments conducted by Wainman et al. (1987), Zhao et al. (1997) and Choe et al. (2018) were considered for this purpose and successfully validated the modelling techniques.

3.1 Zhao et al. (1997)

Out of fourteen experiment test specimens of Zhao et al. (1997), Test 1 was adopted for the validation purpose. The details of the composite beam are IPE 300 steel beam with 25 mm thick mineral wool used as fire protection. The Fig. 4(a) and (b) shows the

comparison of the steel bottom flange temperature and midspan deflection of the model with experimental results.

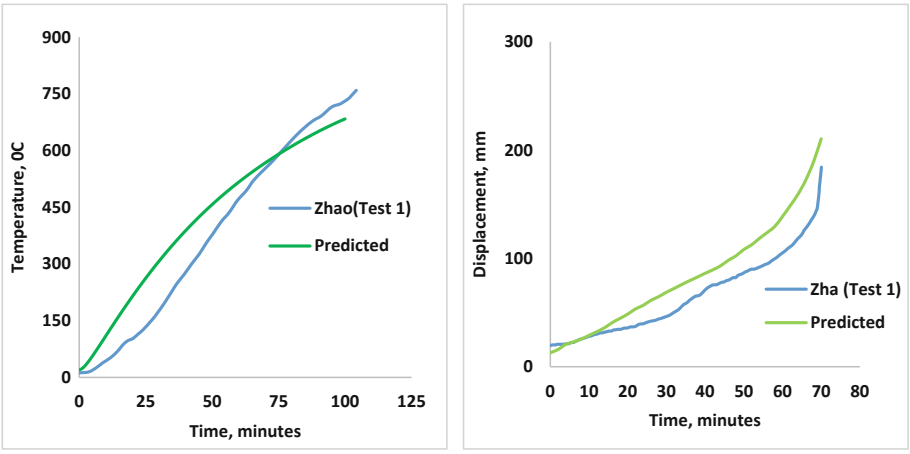

Fig. 4. Bench marking of model with experimental data Test1 (Zhao et al. (1997)) (a)steel bottom flange temperature (b) mid span deflection.

3.2 Wainman and Kirby (2018)

From Wainman and Kirby test series, Test 15 from Wainman et al. (1987) was considered for validation. Figure 5 shows the isometric view of the model in Abaqus. User subroutine was adopted to incorporate the temperature in each and every node of the beam, and it was coupled with the subsequent stress analysis. The temperature distribution on the steel bottom flange and midspan deflection of the composite beams were compared with the literature data, as shown in Fig. 6(a) and (b), respectively, which shows a very good agreement.

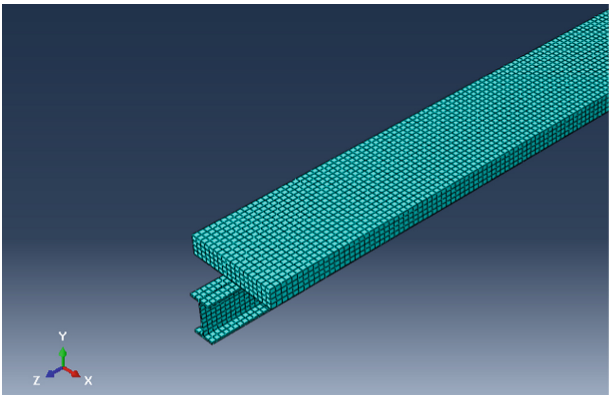

Fig. 5. Model in Abaqus.

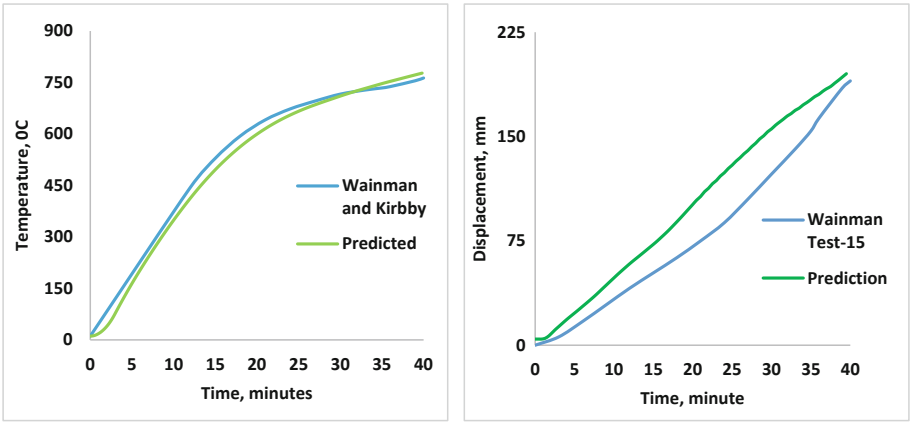

(a) (b)

Fig. 6. Bench marking of model with experimental data Test 15 (Wainman et al. (1987)) (a)steel bottom flange temperature (b) mid span deflection.

3.3 Choe et al. (2018)

Choe et al. (2018a and b) conducted a series of fire test on a 12.8 m long composite beam with different parameters. Test-3 from this experiment series was considered for validation purpose. The steel beam used in the experiment was of size W18 × 35. Lightweight profiled concrete slab of width 1.83 m with metal deck was used. At both ends of the beam, four 12.7 mm diameter reinforced bars of yield strength 415 MPa were used as hogging reinforcement. These reinforcements were extended beyond the slab and tied to the supporting system to simulate the continuity of rebar. Cementitious gypsum-based fire protection of thickness 16 mm was used throughout the steel beam length. The isometric view of the beam and the close view of the connection are shown in Fig. 7(a) and (b). To achieve the nodal temperature history during elevated temperature, a subroutine was adopted while executing heat transfer analysis. Figure 8 shows the comparison of the temperature distribution of steel beam and concrete slab of the model with literature.

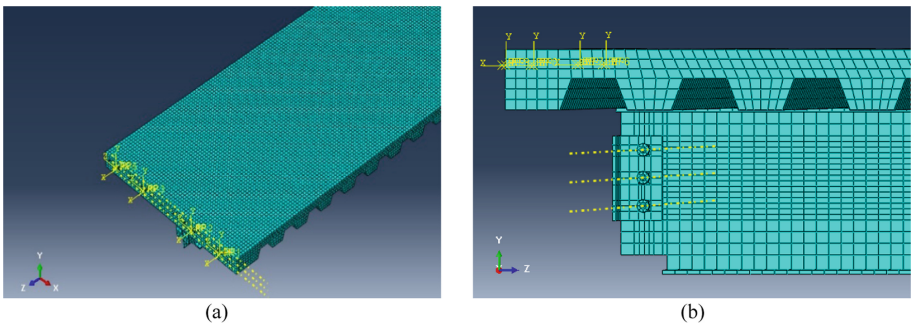

(a) (b)

Fig. 7. (a) Isometric view of the model in Abaqus (b) details of connection.

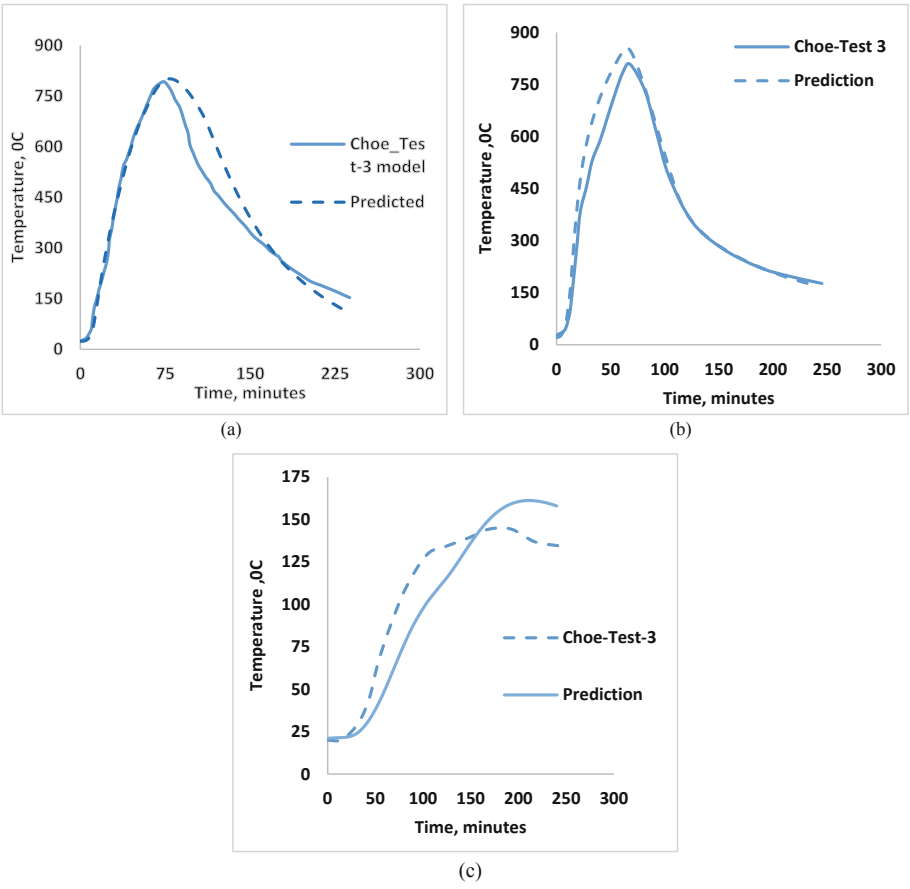

Fig. 8. Bench marking of model with experimental data Test 3 (Choe et al. (2018) (a) steel beam bottom flange temperature (b) Bottom concrete slab temperature distribution (c) Top concrete slab temperature distribution.

The vertical load was given in stress analysis as the first step. A total vertical load of 106 kN was applied at six equally spaced points. The thermal load was applied in the second step. In the numerical model, axial restraint offered by the support was modelled using connector elements available in the interaction module of Abaqus. The buckled shape of the prediction is shown in Fig. 9. The gravity load was removed in the experiment once the midspan deformation exceeds the allowable limit of L/20. A similar procedure was adopted in the numerical model as well. Figure 10(a), (b) and (c) shows the benchmarking of the model developed with the experimental results of midspan deflection Vs. Time and Rebar force Vs. Time.

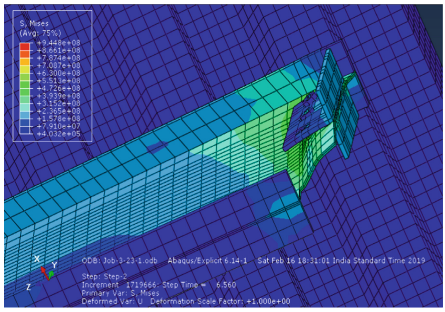

Fig. 9. Buckled shape of the specimen in Abaqus model.

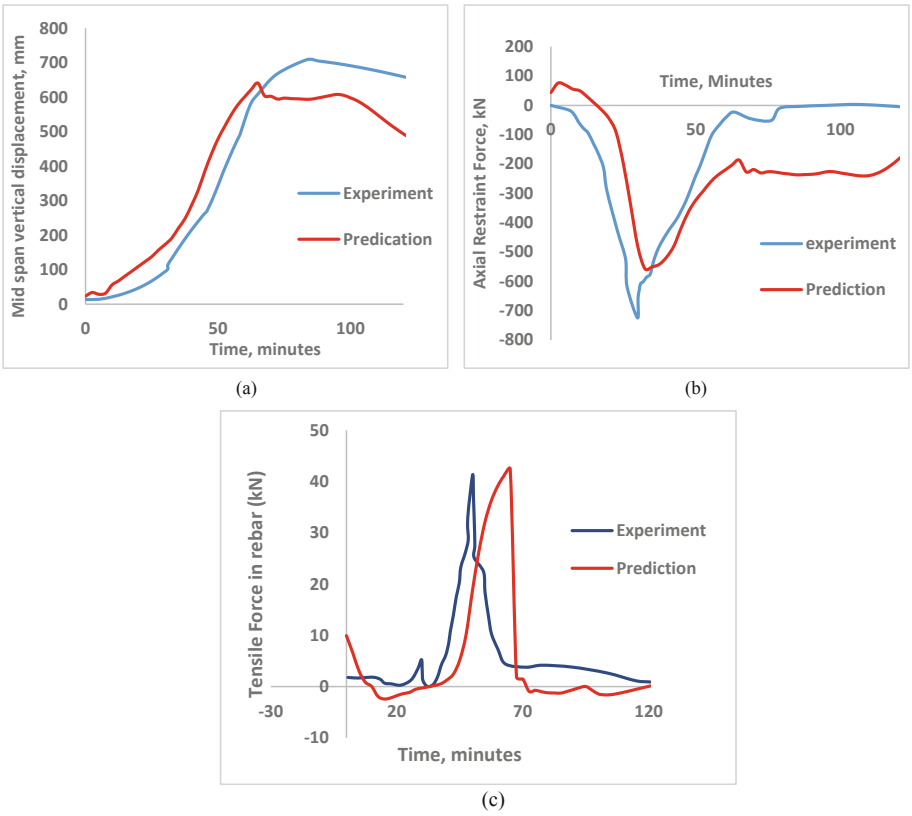

Fig. 10. Bench marking of model with experimental data Test 3 (Choe et al. (2018) (a) Mid span deflection (b) Axial restraint force (c) Tensile Force in rebar.

4 Parametric Study

A detailed parametric study was carried to comprehend the roles of various parameters on the behaviour of the long-span continuous composite beam. The details of the various parameters considered in this paper are listed in Table 1.

Table 1. Models details considered for the analysis

S. No.	Model name	Parameters
1	**CBSS1**	Stiffness of the supporting system: 22 kN/mm
2	**CBSS2**	Stiffness of the supporting system: 110 kN/mm
3	**CBSS3**	Stiffness of the supporting system: 220 kN/mm
4	**CBSS4**	Stiffness of the supporting system: 2200 kN/mm
5	**CBSS5**	Lateral Stiffness of the supporting system: Infinity
6	**CBP**	Composite beam without any rebar in hogging moment region
7	**CBHR**	Composite beam with rebar in hogging moment region
8	**CBRS1**	Stiffness of Rebar support 14 kN/mm
9	**CBRS2**	Infinity

4.1 Effect of Stiffness of the Supporting System

In the experiment of Choe et al. (2018), the axial restraint stiffness of the supporting system, which includes column and supporting braces was found to be 220 kN/mm. However, a significantly broad range of end-conditions may prevail in real-time structures. To understand the effect of the axial restraint on the behaviour of the member, five models with different stiffness values as listed in Table 1 (Serial Numbers 1 to 5) have been modelled and studied the behaviour under fire loading. CBLS3 was assigned with stiffness used in the experimental setup. In models CBSS1, CBSS2 and CBSS4 the stiffness was $1/10^{th}$, half and 10 times of stiffness in the experiment. Whereas in the model CBSS5, the hypothetical rigid condition was considered. The supporting system stiffness was incorporated in the model with the help of connectors. In the model CBSS5 with infinite axial restraint stiffness at support, the buckling of the web and bottom flanges occurred at around 17.5 min after fire loading started whereas in the other models, with stiffness 2200 kN/mm, 220 kN/mm, 110 kN/mm and 22 kN/mm the buckling took place at around 23 min, 30 min, 32.5 min and 40 min respectively. By reducing the axial restraint stiffness of the supporting system, the buckling can be delayed in the beam-web or bottom flange, thereby, potentially increasing the fire resistance of the beam.

The comparison of midspan deflection of various models considered is shown in the Fig. 11. It was assumed that the beam fails when the midspan deflection in the beam reaches 620 mm (L/20). In models CBSS1, 2, 3 and 4, the failure of the beam was observed in between 60 min to 65 min. Whereas in the model CBSS5, the maximum deflection observed was around 600 mm at around 65 min. The restraint force developed in the supporting system increases with the axial restraint stiffness. In the heating phase of the analysis, the beams with more axial restraint stiffness behaved in a better way. The running out failure can be delayed in the members by increasing axial restraint stiffness of the supporting system.

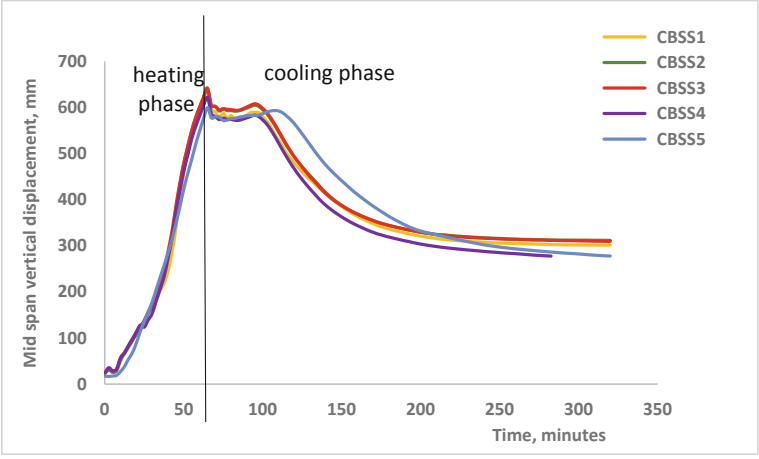

Fig. 11. Mid span deflection.

The stress plots at the connection at around 325 min after staring the analysis is shown in the Fig. 12. In model CBSS5 with rigid connection, during the cooling phase, it was observed that, at around 125 min, the web started yielding near the connection and axial force demand in the connection increased in a faster way compared to other models, which leads to changing of the nature of force demand from compression to tension. The axial restraint force at the connection is shown in the Fig. 13. It may cause the failure of the connection in the cooling phase. Whereas the models with less lateral stiffness, the tensile force demand in the connection during cooling phase was negligible. However, a more detailed parametric study is required by changing various parameters to understand the behaviour.

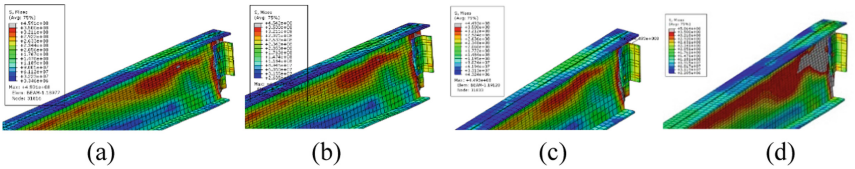

Fig. 12. Stress fields for models (a) CBSS1 (b) CBSS2 (c) CBSS3 and (d) CBSS5 at 325 min.

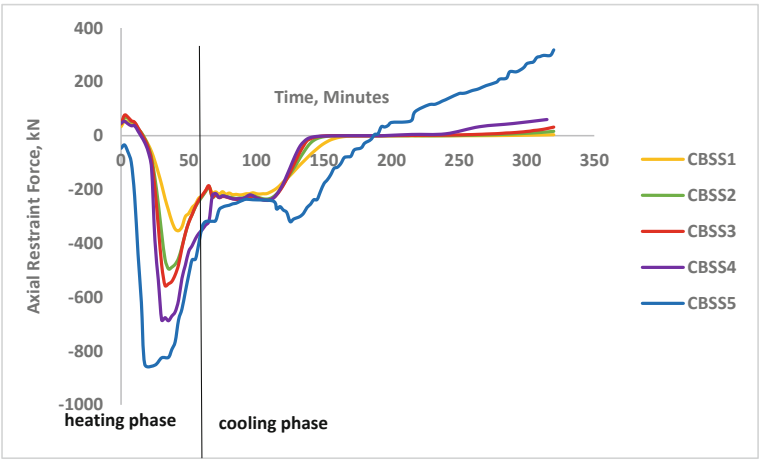

Fig. 13. Axial restraint force.

4.2 Effect of Bond Strength of Negative Reinforcement at Support

In the experiment, it is reported that the rebar bond with concrete was lost during heating phase itself. Furthermore, the failure of the bond in the experiment happened well before reaching its theoretical bond strength. In this paper, the authors attempted to understand the behaviour of the beam, assuming the bond failure is not happening in the member. Analyses listed in serial numbers 6 and 7 studied the effect of negative reinforcement at the support. The model CBP was without any additional reinforcement in the hogging moment region, and the model CBHR was with some reinforcement in the hogging side. The comparison of midspan deflection of the beam is shown in Fig. 14(a). It is evident that the beam with hogging moment reinforcement at the support, the peak deflection has reduced from 866 mm to 640 mm. The axial force developed at the support is shown in Fig. 14(b). The behaviour is more or less the same until 50 min. At around 50 min, there was a sudden rise in the deflection for the model CBP. Whereas in the beam CBHR, the rate of increase of deflection is comparatively slow, and it is due to the presence of reinforcement bars in the hogging side of the member. If we compare the axial force demand in the cooling phase, the tensile force in the connection is more for CBP compared to CBHR, which may cause the welded connection failure by rupture of the weld.

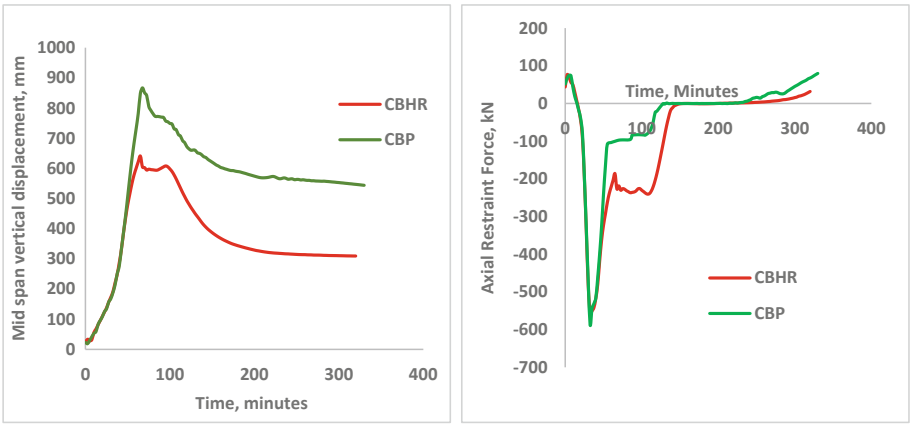

(a) (b)

Fig. 14. (a) Mid span deflection (b) Axial restraint force.

4.3 Effect of Continuity of Negative Moment Reinforcement at the Support

The beam models listed in Table 1 with serial numbers 8 and 9 were analysed to study the effect of continuity of negative reinforcement in the long span composite beam. In the beam CBRS1, the experimental support condition was given. In the experiment, to simulate the continuity condition, the rebars were extended beyond the slab ends and tied to a hollow beam. In numerical modelling, the support condition was modelled with the help of connectors. The stiffness of the supporting system was calculated and assigned to the connector. In real-time, the rebar will be embedded in concrete, and it will be continued in the adjacent concrete slab. Therefore, specimen CBRS2 was modelled with the axial stiffness of supporting member as infinity. Remaining all parameters such as dimensions of various parts, boundary conditions, fire loading, gravity loading pattern were kept as same as mentioned in the literature. It was found that in the beam CBRS2, the peak midspan deflection gets reduced to 610 mm in comparison to 645 mm with the beam CBRS1 as shown in the Fig. 15(a). Axial forces developed in the rebar of various models are plotted in the Fig. 15(b). During the cooling phase, the compressive force was developed in the rebars of model CBRS2, which further slowdown the deflection recovery of the beam.

The axial restraint force developed at the support is plotted in Fig. 16. At around five minutes after the thermal loading, the steel beam expands, and it comes in contact with the supporting system. Further, the expansion is stopped by the support by offering compressive force induced at the support. The peak axial force developed at the support gets reduced from 556 kN to 505 kN when the stiffness of the rebar end support changed from 14 kN/mm to infinity. It is due to the additional compressive force developed in the rebar.

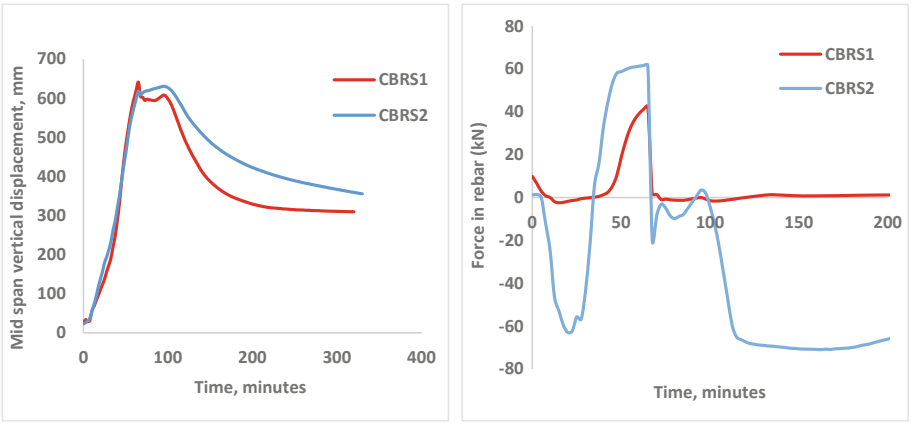

(a) (b)

Fig. 15. (a) Mid span deflection (b) Tensile Force in rebar.

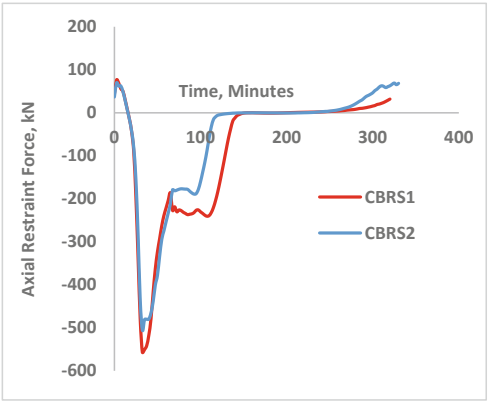

Fig. 16. Axial restraint force.

5 Conclusions

A three-dimensional model was successfully developed for simulating the behaviour of steel concrete composite beam under elevated temperature using the finite element tool Abaqus. All the components were modelled using solid elements and it is able to predict the behaviour of beam in an accurate way. The procedure of modelling and analysis was validated with experimental data. The beam was subjected to a loading of 45% of its ultimate capacity, one hour fire loading and subsequent cooling phase. The influence of reinforcement in the hogging zone of the beam, stiffness offered by the supporting column and the influence of the continuity of the reinforcement at support were studied in this paper. The double angle connection bolted to the beam and welded to the column was used for all models. The stiffness of the supporting system plays a major role during the cooling phase of loading. As the stiffness of the supporting system increases, the

tensile force developed in the connection increases, which may even cause the failure of weld during cooling phase. The flexural strength of the beam during heating phase can be increased by providing additional reinforcements in the hogging moment region of the beam near support and thereby avoid the runout failure of the member during heating phase of loading. Detailed study is required for confirming the findings.

References

Agarwal, A., Selden, K.L., Varma, A.H.: Stability behaviour of steel building structures in fire conditions: role of composite floor system with shear-tab connections. J. Struct. Fire Eng. **5**(2), 77–96 (2014). https://doi.org/10.1260/2040-2317.5.2.77

Agarwal, A., Varma, A.H.: Fire induced progressive collapse of steel building structures: the role of interior gravity columns. Eng. Struct. **58**, 129–140 (2014). https://doi.org/10.1016/j.engstruct.2013.09.020

Agarwal, A.: Stability of steel building structures under fire loading. PhD dissertation. School of Civil Engineering, Purdue Univ. (2011)

Agarwal, A., Varma, A.H.: Design of steel columns at elevated temperatures due to fire: effects of rotational restraints. Eng. J. AISC **48**, 297 (2011)

Cedeno, G., Varma, A.H., Agarwal, A.: Behaviour of floor systems under realistic fire loading. In: Proceedings on CD-ROM of the ASCE Structures Congress, ASCE, Reston, VA, pp. 1–10 (2009). https://doi.org/10.1061/41031(341)224

Choe, L., Agarwal, A., Varma, A.H.: Steel columns subjected to thermal gradients from fire loading: experimental evaluation. J. Struct. Eng. (United States), **142**(7) (2016)

Choe, L., et al.: Fire performance of long-span composite beams with gravity connections. In: Proceedings of the 10th International Conference on Structures in Fire Fire SERT, Ulster University, Belfast, UK, 6–8 June 2018

European Committee for Standardization (CEN): Eurocode 4: Design of Composite Steel and Concrete Structures, Part 1–2: General Rules – Structural Fire Design. European Committee for Standardization, Brussels (2005)

European Committee for Standardization (CEN) (2002), Eurocode 1: Actions on Structures, Part 1.2: General Actions – Actions on Structures Exposed to Fire. European Committee for Standardization (2002)

Fischer, E.C., Varma, A.H., Agarwal, A.: Performance-based structural fire engineering of steel building structures: design-basis compartment fires. J. Struct. Eng. (United States) **145**(9), 04019090 (2019)

Fischer, E.C., Varma, A.H.: Fire resilience of composite beams with simple connections: parametric studies and design. J. Constr. Steel Res. 119–135 (2016). https://doi.org/10.1016/j.jcsr.2016.08.004

Fischer, E.C., Varma, A.H.: Fire behaviour of composite beams with simple connections: benchmarking of numerical models. J. Constr. Steel Res. **111**, 112–125 (2015). https://doi.org/10.1016/j.jcsr.2015.03.013

Fischer, E.C., Selden, K.L., Varma, A.H.: Experimental evaluation of the fire performance of simple connections. J. Struct. Eng. **143**(2), 04016181 (2017). https://doi.org/10.1061/(ASCE)ST.1943-541X.0001664

Selden, K.L., Fischer, E.C., Varma, A.H.: Experimental investigation of composite beams with shear connections subjected to fire loading. J. Struct. Eng. **142**(2), 04015118 (2015). https://doi.org/10.1061/(ASCE)ST.1943-541X.0001381

Wainman, D.E., Kirby, B.R.: Compendium of UK standard fire test data, unprotected structural steel – 1, Reference Number RS/RSC/S10328/1/98/B, British Steel Corporation (now Corus), Swinden Laboratories, Rotherham (1987)

Zhao, B., Kruppa, J.: Fire Resistance of Composite Slabs with Profiled Steel Sheet and of Composite Steel Concrete Beams, Part 2: Composite Beams. ECSC – agreement No. 7210 SA 509, CTICM, France (1997)
ABAQUS: ABAQUS/Standard Version 6.12 User's Manuals, ABAQUS, Providence, RI (2012)